Pergamon

PII: S0191-8141(97)00005-9

Journal of Structural Geology, Vol. 19, No. 6, pp. 785 to 797, 1997

0191-8141/97 $17.00 + 0.00

The role of veining and dissolution in the evolution of fine-grained mylonites: the McConnell thrust, Alberta

LORI A. KENNEDY* and JOHN M. LOGAN†

Center for Tectonophysics and Department of Geology and Geophysics, Texas A & M University, College Station, TX 77843, U.S.A.

(*Received* 30 *May* 1996; *accepted in revised form* 4 *January* 1997)

Abstract—Microstructural observations of the McConnell thrust fault rocks demonstrate the importance of vein formation and calcite dissolution in the evolution of the McConnell thrust limestone mylonites. The protolith to the mylonite is a micritic limestone. The mylonite contains numerous, discontinuous, bedding-parallel calcite veins that range from relatively undeformed (except for twinning and undulose extinction) to highly sheared. The highly sheared veins show evidence for dynamic recrystallization and grain-size reduction along grain and twin boundaries that can lead to complete recrystallization to a grain size of approximately < 1–3 μm. The bulk of the calcite matrix within the McConnell thrust mylonite is interpreted to have formed by dynamical recrystallization of veins. The emplacement of relatively coarse-grained veins promoted the activation of dislocation creep within the fault rocks of the thrust. In the absence of the increase in grain size afforded by vein emplacement, it is anticipated that the fine-grained protolith would have deformed predominantly by solution transfer (with grain-boundary sliding) and localized, brittle shearing. The layer-parallel calcite veins are found in close proximity to sheared clay seams which are interpreted to represent the insoluble residue left behind after dissolution of calcite. These clay seams may have contributed to the build up of high pore fluid pressures which, if intermittently reaching lithostatic conditions during displacement, would result in transient brittle failure and thrust-surface-parallel vein emplacement in an otherwise ductilely deforming rock. © 1997 Elsevier Science Ltd

INTRODUCTION

The development and behaviour of fault zones is significantly influenced by the infiltration of fluids during deformation. Such fluid–rock interactions can produce either weakening (strain softening) or strengthening (strain hardening) of fault zones. Fault-zone weakening may occur by several processes including: (1) reduction of the normal effective stress as a result of high pore fluid pressures acting on a fault (e.g. Hubbert and Rubey, 1959; Byerlee, 1990; Blanpied *et al.*, 1992); (2) reaction softening, primarily in the form of retrograde mineral reactions (e.g. White and Knipe, 1978); (3) hydrolytic weakening of minerals (e.g. Kronenberg, 1994 and references therein); and (4) grain-size-dependent processes such as solution transfer, which, under certain circumstances, may operate under lower differential stresses than that required for dislocation creep or cataclasis (e.g. Rutter, 1976; Schmid, 1976; Rutter and Mainprice, 1979; Wojtal and Mitra, 1986; Walker *et al.*, 1990; Wojtal, 1992). However, solution-transfer processes may also act to increase the strength of faults by crack healing and the precipitation of cement (e.g. Stel, 1981; Angevine *et al.*, 1982; Wojtal and Mitra, 1986; Chester and Higgs, 1992; Fredrich and Evans, 1992). This study examines the role of fluid–rock interactions, in particular those of fluid-assisted diffusion processes and high pore fluid pressures, on the microstructural development of fine-grained calcite mylonites found in the foreland of fold-and-thrust belts.

The deformation microstructures observed in both naturally and experimentally deformed calcite mylonites developed from coarse-grained marbles are well documented (e.g. Schmid *et al.*, 1981; Vernon, 1981; Behrmann, 1983; Heitzmann, 1987; Schmid *et al.*, 1987; Van Der Pluijm, 1991; Lafrance *et al.*, 1994; Busch and Van Der Pluijm, 1995). In general, these studies indicate that at low temperature and sufficient levels of differential stress, coarse-grained calcite deforms initially by twinning on *e*-planes, and that with increasing temperature, *r*-slip dominates, followed by dynamic recrystallization and a concurrent decrease in grain size. Deformation of fine-grained limestone (or the crushed gouge equivalent) has also been studied both in the laboratory (e.g. Schmid *et al.*, 1977, 1981; Friedman and Higgs, 1981; Walker *et al.*, 1990) and, more rarely, in natural deformed limestones (Dietrich and Song, 1984; Burkhard, 1990). Deformation mechanism maps, derived from deformation experiments, suggest that under a wide variety of geological conditions, deformation of fine-grained limestones may be dominated by grain-size-sensitive creep such as solution transfer and grain-boundary sliding (e.g. Rutter, 1976; Schmid *et al.*, 1977; Walker *et al.*, 1990). However, field observations demonstrate the key roles played by fluid–rock interactions and secondary phases on deformation processes in fault rocks.

The mylonite sampled for this study comes from the exposure of the McConnell thrust at the base of Mt Yamnuska, Alberta (Fig. 1). The deformation mechan-

*Present address: Earth and Ocean Sciences, 6339 Stores Road, University of British Columbia, Vancouver, B.C., Canada, V6T 1Z4.

†Present address: Pacific Institute for Crustal Studies, P.O. Box 1776, Bandon, OR 97411, U.S.A.

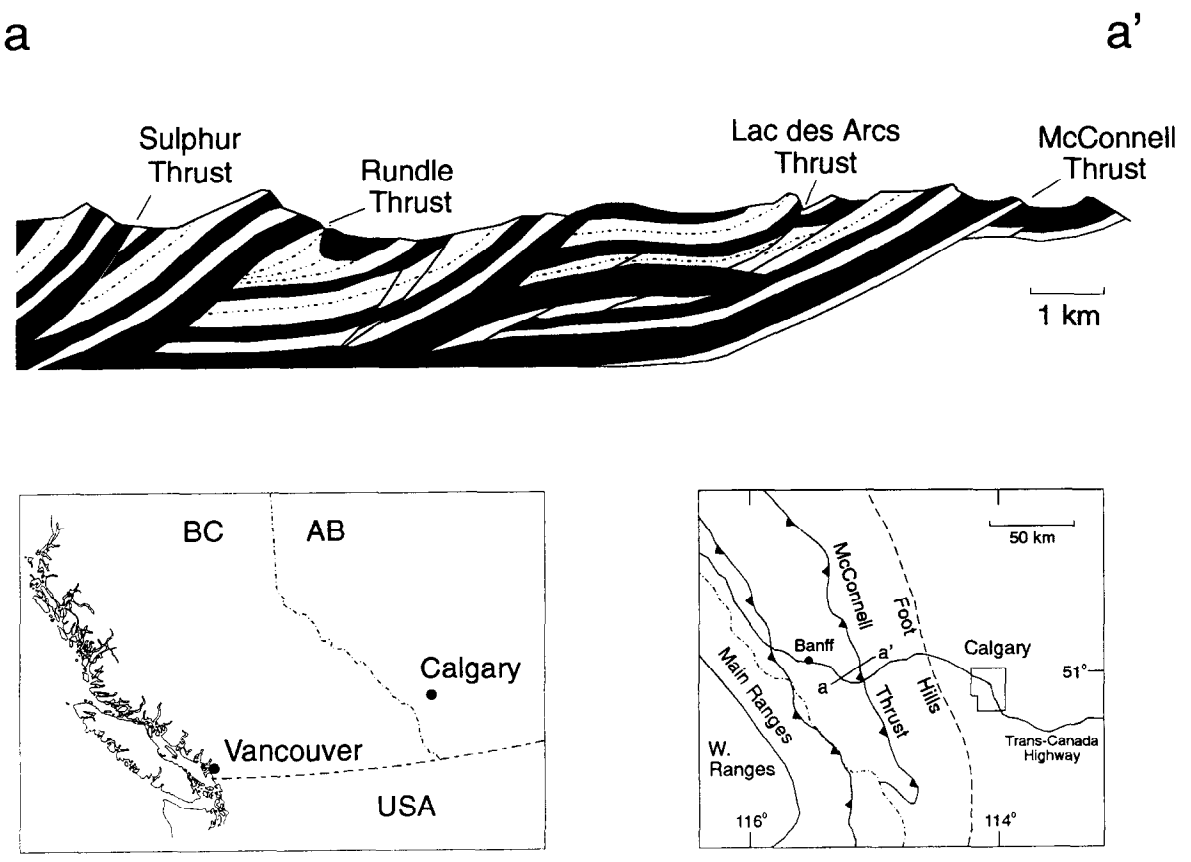

Fig. 1. Location maps and cross-section through the foreland of the Canadian Rockies. Field area for this study is the most easterly portion of the McConnell thrust, the geometry of which is an upper flat of the thrust fault, located at Mt Yamnuska. (Modified from Bradbury and Woodwell, 1987.)

isms operative during formation of the mylonite are inferred from the microstructures of the McConnell thrust calcite mylonite, described herein. The microstructural evolution of the McConnell thrust mylonite can then be placed in a geological framework in which the presence of a weak basal layer is a mechanical necessity, that is at the base of a large foreland thrust sheet (e.g. Hubbert and Rubey, 1959; Chapple, 1978; Davis *et al.*, 1983; Wojtal and Mitra, 1986; Burkhard *et al.*, 1992).

GEOLOGICAL SETTING AND MESOSTRUCTURES

The McConnell thrust represents the easternmost expression of the Front Ranges of the Canadian Rocky Mountains (Fig. 1). On a regional scale, the McConnell thrust is listric, dipping southwest at a low angle, with a transport direction towards ~063° (Spang *et al.*, 1981). Mt Yamnuska represents the 'upper flat' geometry of a well-developed ramp–flat structure of the McConnell thrust. The contact between the hanging wall Eldon Formation limestones and footwall Belly River Formation shale and sandstones is locally well exposed along the upper flat (Fig. 2a). Thrusting in the adjacent foothills has been placed between 65 and 60 Ma (Elliott, 1976). The foothill thrusts post-date the McConnell thrust and thus indicate that the McConnell thrust ceased activity by ~65 Ma. Recent K–Ar dating on illite–illite/smectite clays taken from the fault gouge, date deformation at ~77 Ma, which is interpreted to represent the age of the main episode of movement (Covey *et al.*, 1994). Based on cross-section reconstructions, the McConnell thrust has a minimum displacement of ~20 km and a maximum displacement of ~40 km (e.g. Price and Mountjoy, 1970). Therefore, the McConnell thrust was translated upwards of ~40 km over a period of ~12–17 million years, giving rise to about a 3 mm/year average rate of displacement.

Temperatures during deformation are not well constrained (Woodwell, 1985). Cross-section reconstructions place *maximum* burial depths (i.e. depth of the lower flat) of the thrust at 8–10 km during thrusting (Elliott, 1976), which, assuming a 25°C/km geothermal gradient, gives rise to maximum temperatures on the order of 200–250°C. However, during displacement, the McConnell thrust continually ramped up-section to the present location at Mt Yamnuska, which was most likely not buried more than 4–5 km during displacement. Vitrinite reflectance data of Bustin (1983) indicate that, at Mt Yamnuska, temperatures of the underlying Belly River Formation were probably about 140°C. The

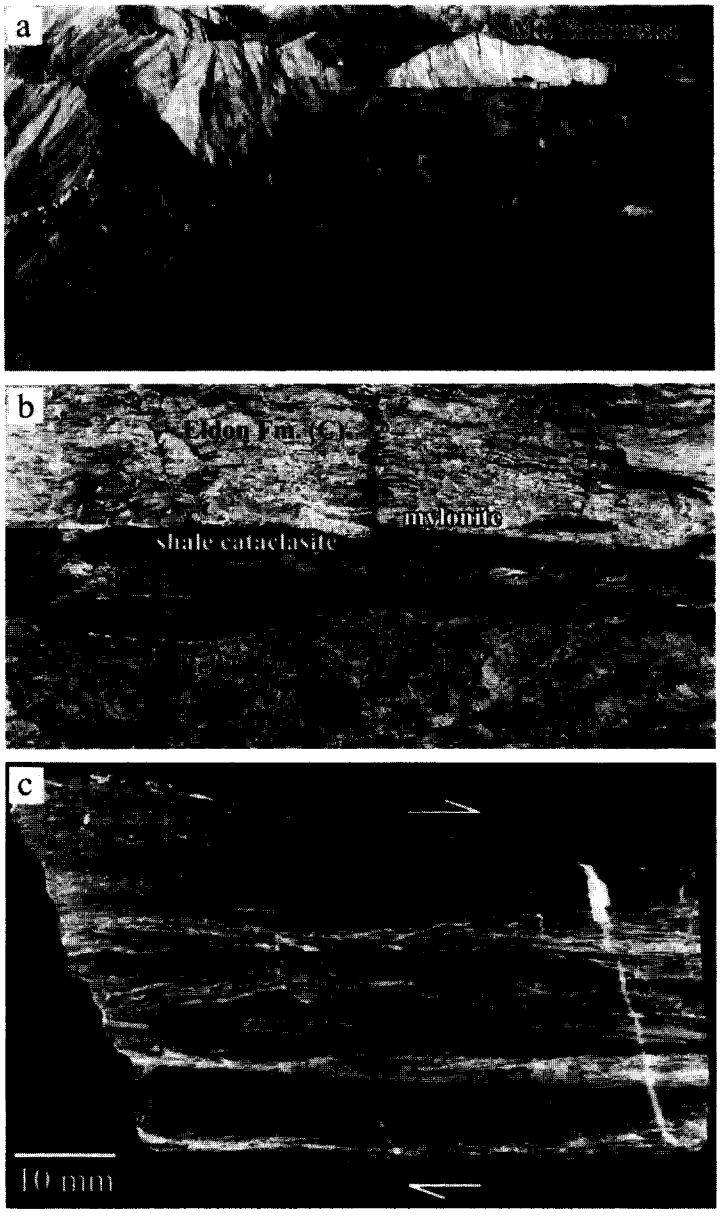

Fig. 2. (a) Aerial view of the McConnell thrust. Middle Cambrian Eldon Formation limestones override Cretaceous carbonaceous shales and sandstones of the Belly River Formation. Horizontal length of Mt Yamnuska is about 800 m. Dashed line represents approximate location of thrust ramp and flat. Photo taken by M. Bustin .(b) Close-up of the contact between the hanging wall Eldon Formation limestone and and footwall Belly River Formation shales and sandstones. The limestone mylonite is not easily discerned in the field. Horizontal length of photograph is about 2.5 m. (c) Polished sample of the McConnell thrust calcite mylonite. The light, horizontal layers are enriched in calcite veins and thin dark stringers are enriched in clay minerals and dolomite.

temperatures reflected by the preserved microstructures at Mt Yamnuska are discussed later in the text.

The McConnell thrust is characterized by an extensive damage zone and a fault-zone core, as is common to fault zones in general (e.g. Venter, 1973; Chester and Logan, 1986; Wojtal and Mitra, 1986; Wojtal and Pershing, 1991; Kennedy and Logan, in review). The fault-zone core consists of two distinct fault rocks; a limestone mylonite above and a shale cataclasite below. Although slivers of the underlying cataclasite are thrust into the limestone mylonite, these fault splays are late in the transport history and have not caused substantial mixing (Fig. 2b). In contrast, the boudins of the hanging wall mylonite are incorporated into the footwall cataclasite (Fig. 2b). The fault-zone core is surrounded by a damage zone halo, defined by mesoscopic fracture and fault arrays and folds, within both the hanging wall limestone and the footwall shale, a mesostructure common to many foreland thrust faults (e.g. Wojtal and Mitra, 1986; Wojtal and Pershing, 1991).

The thickness of the hanging wall mylonite ranges from about 40 to 100 cm, and the contact between the mylonite and the hanging wall damage zone is gradational. The *hanging wall damage zone* above the mylonite is characterized by abundant, discontinuous veins and stylolites, and is faulted and folded. The density of veins

that are not parallel to bedding increases noticeably towards the SW (i.e. towards the ramp). The *limestone mylonite* is foliated parallel to bedding, with the foliation defined by alternating, discontinuous, light and dark layers and discontinuous bedding-parallel veins (Fig. 2c). The darker layers are clay-rich seams which vary in thickness from <1 mm to approximately 0.5 cm in thickness. The clay seams are commonly striated with the striations oriented subparallel to the transport direction. Bedding-parallel veins (within the mylonite) are up to ~ 3 mm thick and are commonly fibrous, with the fibres oriented approximately parallel to the transport direction at a small angle to the vein walls. A stretching lineation was not observed. Discontinuous veins and stylolites are abundant in the mylonite and occur at all angles, although most are oriented either parallel, perpendicular or at high angles to bedding. In contrast to the mylonite–hanging wall contact, the contact between the mylonite and the underlying shale cataclasite is sharp and commonly parts upon sampling. This contact has slickensides with striations oriented subparallel to the transport direction.

METHODOLOGY

Oriented samples for this study were obtained from the hanging wall flat region of Mt Yamnuska, in areas where both the limestone mylonite and underlying shale cataclasite were exposed. Samples were collected along several transects across the fault zone (approximately eight samples per transect) from the undeformed protolith to the mylonite. Microstructures were observed from ultra-thin sections under an optical microscope with a cathodoluminescence (CL) attachment, and by transmission electron microscopy (TEM). The TEM used was a JEOL 2012, operated at 200 kV. Changes in mineralogy were determined by X-ray diffraction analyses (XRD).

MICROSTRUCTURES

Optical microstructures

Hanging wall damage zone and protolith. The undeformed hanging wall limestone (protolith to the mylonite) is generally fine grained, ranging from ~ 3 to 10 μm, although grain size varies as a result of burrows and other diagenetic processes. Calcite grain boundaries are commonly serrated in appearance and while the larger grains contain at least one set of twins, smaller grains are usually devoid of twins (Fig. 3a). Undulose extinction is common in all grains. The limestone contains dolomitic patches, and pods and oval-shaped burrows infilled with coarse-grained calcite are common and typically rimmed by 'stylolites'. Consistently, veins are oriented perpendicular to bedding while stylolites are parallel to bedding. Stylolites typically offset veins.

The damage zone of the McConnell thrust is represented by numerous fractures, anastomosing microshear zones, veins and stylolites, and irregular patches of dolomite and clay-rich areas; all of which impart a fragmented, brecciated character to the rock. Bulk cataclasis has not occurred and, although most grains are twinned, there is no evidence for deformation by pervasive dynamic recrystallization of the calcite matrix. The microshear zones are <1 mm in thickness and exhibit extreme grain-size reduction. Within these microshear zones, the larger calcite grains have bent twins, but the fine-grained calcite is not twinned; rather, the grain boundaries are serrated and lobate. Insertion of a gypsum plate demonstrates that a crystallographic preferred orientation (CPO) was not developed within the microshear zones. Under cathodoluminescence, the fine-grained microshear-zone material luminesces slightly brighter than the surrounding limestone. Cathodoluminescence in calcite is thought to be a result of trace amounts of Mn^{2+} (activating ion) vs Fe^{2+} (quenching ion) in the crystal lattice (Marshall, 1988). Where fractures and microshear zones luminesce differently to the matrix, we infer that either fluid with different proportions of Mn and Fe than the matrix infiltrated the rocks preferentially along these zones, or that infiltrating fluids altered the trace-element composition of the rocks (e.g. Newman and Mitra, 1995).

Fractures, veins and stylolites occur at all angles to the thrust surface: stylolites are not consistently oriented at approximate right angles to veins. Rather, stylolites may occur parallel to vein walls and other 'rigid' objects, such as dolomitized worm burrows (Fig. 3b). Stylolites offset veins and are also cross-cut by calcite veins, although the latter is more common. Areas enriched in clay minerals and dolomite are common and the amount of dolomite–clay-rich areas varies considerably along strike of the McConnell thrust, ranging from rare up to $\sim 10\%$ of a thin section. The origin of the dolomite–clay-rich areas is addressed later in the text. Calcite veins almost always exhibit deformation, ranging from undulose extinction, to intense twinning, to subgrains.

Limestone mylonite. The limestone mylonite possesses a distinct foliation defined by alternating layers of dynamically recrystallized calcite ('matrix'), thin discontinuous dolomite–clay-rich layers (herein termed 'clay seams') and bedding-parallel calcite veins (Fig. 3c). The recrystallized matrix is cross-cut, generally at high angles, by a myriad of irregular and discontinuous calcite veins (Fig. 4a–d).

The bedding-parallel veins range from texturally undeformed (except for twinning and undulose extinction of the calcite grains) and coarse grained (>400 μm), to sheared and dynamically recrystallized, ultimately reaching grain sizes of less than ~ 1 μm. In many cases, the remnants of calcite veins are demonstrably incorporated into and contribute to the recrystallized 'matrix'.

Fig. 3. (a) Photomicrograph of limestone protolith taken from the top of Mt Yamnuska. Many calcite grains are twinned, show undulose extinction, and have irregular and serrated grain boundaries. These features are probably sedimentary in origin. (b) Damage zone of the hanging wall. Veins, stylolites, microshear zones and twins in calcite are abundant. Overall, the damage zone has the appearance of a rock deformed by primarily brittle processes, accompanied by solution transfer. Arrows point to a stylolite that occurs both parallel and perpendicular to a vein. Sense of shear: top-to-the-right. (c) Photomicrograph of the mylonite. The foliation is defined by alternating veins and clay seams and also by elongated 'matrix' calcite grains. The 'X' denotes the general area of enlargement for photomicrograph (d). (d) Photomicrograph illustrating the sheared and recrystallized veins (V) that comprise a significant portion of the matrix. This photograph is a close-up of the general area marked by an 'X' in photomicrograph (c). (e) Dynamically recrystallized matrix. Larger grains are elongate, twinned, show undulose extinction and have serrated boundaries. Smaller grains are commonly optically strain free. A relatively undeformed vein parallels the bottom of the page. Sense of shear: top-to-the-right. (f) Photomicrograph showing dynamically recrystallized grains (subgrain migration, little arrow) and coarser grains undergoing twin boundary migration (big arrow). Sense of shear: top-to-the-right.

Although these veins are nearly completely recrystallized, all portions of the former vein show qualitatively (by insertion of a gypsum plate) similar CPOs. Similar features to these have been described by Burkhard *et al.* (1992) from calcite mylonites developed along the Glarus Nappe in the Swiss Alps.

Distinguishing the initial matrix calcite (i.e. calcite inherited from the micritic protolith) from former veins which now compose a portion of the matrix is difficult; a significant portion (all?) of the 'matrix' consists of fine-grained, presumably dynamically recrystallized, vein calcite that was introduced earlier in the transport history of the McConnell thrust. In fact, there appears to be a complete transition from coarse-grained, layered, areas which are clearly veins, to elongate porphyroclastic areas which are still recognizably sheared veins (Fig. 3d), to areas of nearly complete grain-size reduction by dynamic recrystallization, with rare elongate vein material as the only indication that the fine-grained recrystallized material may have once been a coarse-grained vein. Dynamic recrystallization and grain-size reduction initially occurs along twin boundaries, shear bands and vein boundaries.

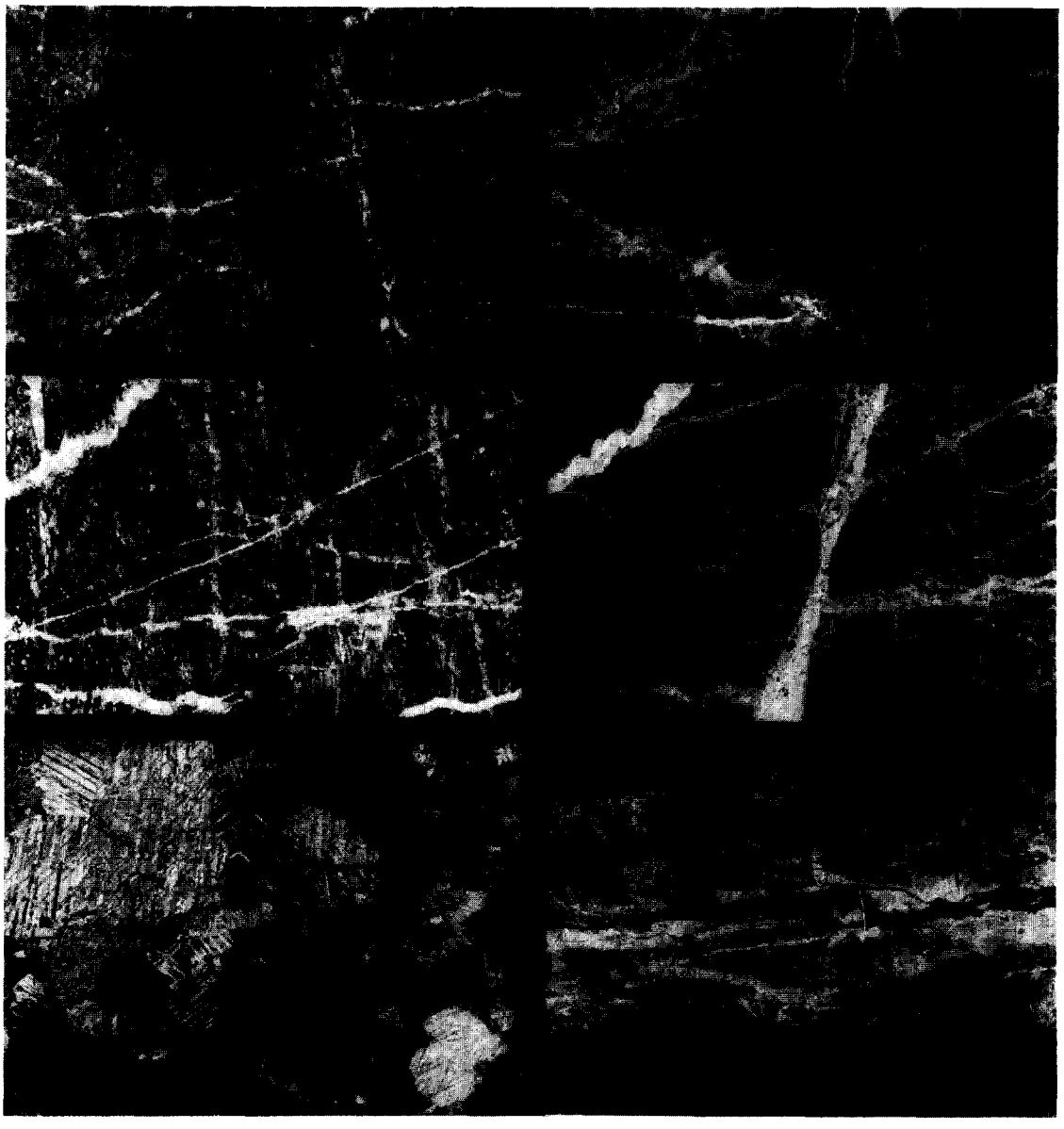

Fig. 4. Optical micrographs (left-hand side) and corresponding cathodoluminescent (CL) images (right-hand side) of the limestone mylonite. (a) and (b) Clay seam and adjacent matrix. Note several thinner 'clay seams' within the matrix. The CL image shows the brightly luminescent material within and parallel to the clay seams and the duller luminescence of some veins and the matrix. Also, veins oriented generally at a high angle to the clay seam are abundant and both cross-cut and are cross-cut by the clay seam. Dark blebs in the CL image represent primarily dolomite, with lesser amounts of opaque minerals and clay minerals. Sense of shear is right-hand side down. (c) and (d) A relatively late microshear zone (cataclastic), oriented at a low angle to the foliation. The microshear zone cross-cuts and is cross-cut by a myriad of veins. CL micrograph illustrates the brightly luminescent material comprising the microshear zone. Again, veins have variable brightness of luminescence, perhaps indicating different fluid migration events. (e) and (f) Blocky vein-calcite which cross-cuts the foliation at a high angle. CL illustrates the planar geometry of the calcite comprising the vein suggesting successive migration of fluids parallel to the crack during vein formation. Arrows in both images are located on the same crack. All scale bars are 200 μm.

Fine-grained recrystallized grains commonly rim coarse grains. With decreasing grain size (primarily by development of subgrains and recrystallization) twins become less prevalent and the grains tend towards equidimensional shapes, with lobate, serrated grain geometries (Fig. 3f) that are interpreted to have developed by grain-boundary migration. Twin morphology varies, ranging from straight twin boundaries, to thick and curved, to irregular boundaries that bulge into the host grain. In many grains the twins are recrystallized, resulting in a trail of small grains within the host grain, features similar to the Type III and IV twin types of Burkhard (1993) (Fig. 3f). *S–C* fabrics are locally present, however; more commonly, the fine-grained, recrystallized calcite does not form a separate shape fabric (i.e. *S*-foliation), rather the grains are elongate subparallel to the clay seams and to other layer-parallel slip surfaces (i.e. *C*-surfaces), and shear bands are present. Untwinned dolomite rhombo-

hedrons are dispersed throughout the recrystallized areas.

The clay seams vary in thickness from about 10 μm to several mm, are discontinuous, irregular in shape and highly sheared (Fig. 4a & b). Sheared calcite veins within the clay seams may be folded and exhibit subgrain development and dynamic recrystallization. Dolomite rhombohedrons are rimmed with calcite, which may be an artifact of pressure solution. Clay seams are typically lined with stylolites and/or thin veins, and the interface between the clay seams and the matrix is commonly a shear surface. The calcite at the edges of clay seams and stylolites luminesces significantly brighter than the surrounding matrix. Again we infer this to be a result of fluid flow parallel to the clay seams which acted either to slightly alter the trace-element composition of the calcite, or to precipitate calcite with a trace-element composition slightly different to that of the host rock (Fig. 4a & b). Within the clay seams, fabric elements may or may not be present. Kinematic indicators are abundant; however, they do not consistently indicate the same shear sense. Discontinuous shear surfaces, composed predominantly of clays, are common within the clay seams (*Y*-surfaces of cataclasites (e.g. Logan *et al.*, 1992) and *C*-surfaces of mylonite terminology (e.g. Lister and Snoke, 1984)). Veins that cross-cut the recrystallized matrix at high angles may also cross-cut the clay seams or are sheared within the seams. Clay seams are commonly bounded laterally by a zone of anastomosing and coalescing fractures and/or faults (Fig. 3c). In this region, lozenge-shaped fragments of recrystallized calcite matrix and calcite veins are separated by thin cataclastic shear zones. These shear zones luminesce brightly, again suggesting that fluids migrated along these zones and either precipitated new calcite or altered pre-existing calcite. The fractured material is eventually incorporated into the clay seams.

The mylonite matrix is also cross-cut by numerous discrete faults, thin cataclastic (?) shear zones, thick, blocky veins oriented approximately perpendicular to the foliation, and discontinuous, irregular, thin veins of all orientations. Thin cataclastic shear zones occur at both low and high angles to the foliation and both cross-cut and are cross-cut by the clay seams and veins. These shear zones luminesce brightly in CL images, again suggesting the effects of the migration of fluids (Fig. 4c & d). Cathodoluminescence also illustrates the extent of wispy veining within the matrix calcite and differing vein compositions. Veins that appear relatively thick and blocky in optical light appear layered under CL observations, presumably reflecting slightly different calcite compositions parallel to the vein wall (Fig. 4e & f). We suggest that these veins formed by crack-sealing processes. Many structures are offset by discrete normal faults with little (sub-mm) displacement along them, and by thin discontinuous stylolites.

These observations lead us to infer the presence of fluids during deformation. The microstructures of the McConnell thrust mylonite are remarkably similar to those of the Glarus thrust calc-mylonites as described by Burkhard (1990) and Burkhard *et al.* (1992).

Mineralogy

X-ray diffraction patterns of whole rock samples of the mylonite are similar to those of the protolith; both contain mostly calcite with minor dolomite. Significantly, however, there is relatively more dolomite and less calcite in the mylonite compared to the protolith. Bulk chemistry of clay seams, by X-ray mapping for Si, Al, Ca, Mg, K and Fe (using both the electron microprobe and the scanning electron microprobe), indicate that the clay seams are composed primarily of dolomite clasts, distended calcite and opaque minerals (pyrite and galena) set in a K–Al–Si-rich matrix (most probably illite).

TEM observations

TEM microstructures within the mylonite comprise subgrains and recrystallized grains (Fig. 5a & e), deformation twins, areas of high dislocation densities, and euhedral precipitates of calcite and stylolites. These microstructures are common in both the fine-grained and coarse-grained matrices. Areas of high dislocation densities are heterogeneously distributed, and found in both recrystallized grains and in twinned volumes. Most twins possess variable densities of glide dislocations within the twinned volume. Also, the sharpest twins cross-cut most features. For example, dislocation walls are cross-cut by twins (Fig. 5b). Many deformation twin boundaries are irregular in shape and are commonly defined by well-developed dislocation networks or closely spaced arrays of twinning dislocations (Fig. 5c & d). Barber and Wenk (1979) demonstrated that shear on these boundaries necessarily accompanies twinning in order to relax the stresses produced by the shape change on twinning at the surfaces of the lamellae. The irregular shape to twin boundaries indicates that these boundaries have migrated after their formation (e.g. Vernon, 1981; Rutter, 1995).

Stylolites and veins demonstrate the activity of solution-transfer processes within the mylonite. TEM observations show that calcite grains, which are twinned and contain high densities of dislocations, impinge upon linear bands of clay minerals, presumably representing microstylolites (Fig. 5f). Meike and Wenk (1988) also found that preferential dissolution of calcite and subsequent stylolite formation occur in the vicinity of highly deformed calcite grains. Fine-grained, euhedral clay lathes, which probably precipitated from solution, also contribute to the stylolites. The clay aggregates are localized on cracks; however, it is not clear if the cracks formed before or after stylolite development. Solution transfer is also evident by the abundance of euhedral precipitates of calcite. Very few euhedral grains are strain free (i.e. dislocation free), and many contain dislocation

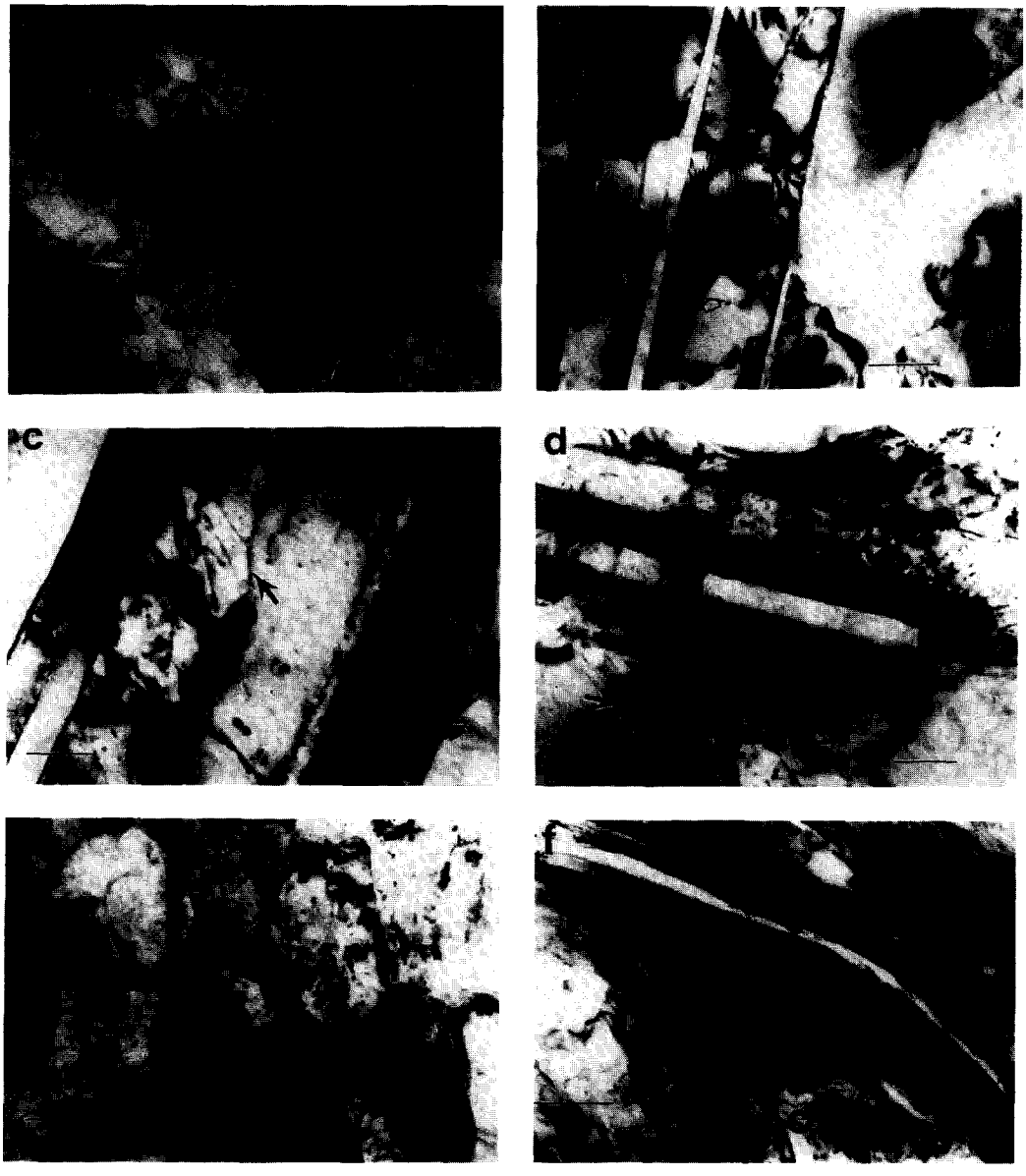

Fig. 5. Transmission electron microscope (TEM) images of the McConnell thrust mylonite. All scale bars are 100 nm. (a) Partially recrystallized fine-grained matrix. Thick arrow points to an example of bulge nucleation of a grain. Thin arrow points to an early, subsequently deformed twin. (b) Twins in calcite. Twin boundaries are straight and sharp and overprint low-angle boundaries (see arrow). Dislocations are present in both the twinned and untwinned portions of calcite. (c) Deformation twins with irregular twin boundaries. The irregularity of twin boundaries suggests that the twins have migrated (arrows). Twins contain many dislocations and twin boundaries are lined with dislocation arrays. (d) Precipitation of calcite (arrow) and deformation twins. Spotted appearance is a result of beam damage. (e) Dynamically recrystallized calcite. Vestiges of planar boundaries (twins?) can be seen in the photograph. (f) Solution seam (stylolite) in the mylonite. Calcite crystals adjacent to the clay aggregate commonly contain high dislocation densities ('C' in photograph). Some of the clay minerals may be precipitates and not just residual minerals.

tangles, suggesting that dislocation glide operated after or in tandem with solution-transfer processes during deformation. There is a notable lack of microcracks within the mylonite matrix at the TEM scale. However, this may simply reflect the fast healing rate of cracks in calcite aggregates (e.g. Olgaard and Evans, 1988).

TEM microstructural observations of the limestone from the McConnell thrust damage zone show evidence for deformation by twinning and minor subgrain development. In common with the mylonite, twins occur both straight and irregular in shape. Subgrains are present but fully recrystallized grains were not observed.

DISCUSSION

Deformation mechanisms

Deformation mechanisms operative during displacement along the McConnell thrust may be inferred from

the observations of the deformation microstructures made at the optical and TEM scales. From these observations it is interpreted that displacement along the McConnell thrust was accommodated by several deformation mechanisms including twinning, dislocation creep, solution transfer (± grain-boundary sliding) and cataclasis; the dominant deformation mechanism probably varied temporally and spatially during thrusting (see below).

Within the hanging wall, above the damage zone, stylolites and veins are oriented parallel and perpendicular to bedding, respectively. These stylolites may be a result of burial, where stylolites are known to propagate parallel to the least principal stress (σ_3), or they may be formed in response to the passage of the hanging wall over the ramp—in either case, the stylolites are not considered to be directly related to the basal shear zone. Calcite grains in the fine-grained protolith commonly have serrated grain boundaries and irregular twins, with no accompanying CPO, and these features are interpreted to be artifacts of diagenesis. Thus, the presence of serrated grain boundaries within fine-grained calcite cannot always be interpreted as a result of dynamic recrystallization. Burkhard (1990) noticed similar features in undeformed limestone from Mesozoic limestones in the Helvetic ranges of western Switzerland and concluded that grain-boundary textures should not be used, on their own, as indicators of deformation mechanisms in fine-grained limestones.

Within the damage zone calcite is invariably twinned and shows undulose extinction, indicating operation of dislocation glide; although the lack of a CPO suggests that neither dislocation glide nor twinning accommodated significant (< 10%) strain. The abundance of veins and stylolites in the damage zone indicates the operation of fracturing and solution-transfer processes. In contrast to the protolith, stylolites are not consistently oriented parallel to bedding and perpendicular to veins. Rather, stylolites occur both perpendicular and parallel to veins, and also form around irregular dolomite blebs. Therefore, in common with other structures, the stylolites probably formed in response to the local environment (or were influenced to local anisotropies), which is not necessarily comparable to the regional stress regime (e.g. Jiang and White, 1995). It is difficult to determine whether the abundant microshear zones within the damage zone deformed by dislocation creep or by cataclasis. The lack of a CPO may indicate deformation by cataclasis with readjustment of grain boundaries by solution-transfer processes: CL illustrates that these narrow zones acted as conduits to fluids. In summary, the damage zone shows structures (at both the meso- and microscale) which indicate that the bulk of the deformation was accommodated by brittle processes, primarily sliding along discrete shear surfaces, operating in tandem with solution-transfer processes. Crystal-plasticity, although active, did not significantly contribute to the overall strain.

In contrast to the damage zone, the McConnell thrust mylonite shows evidence for extensive operation of dislocation creep. However, twinning, cataclasis and fluid-assisted diffusion processes (and grain-boundary sliding?) are also evident. Both the fine-grained and coarse-grained calcite matrix of the mylonite show microstructures indicative of dislocation creep, including bulbous, serrated grain boundaries, reduction of grain size and, at the TEM scale, bulge nucleation and grain boundaries meeting at triple junctions. In contrast to TEM observations, the smallest recrystallized grains commonly appear strain free at the optical level. Therefore, it is difficult to determine whether grain-boundary sliding accommodated significant strain during displacement before the onset of crystal-plasticity, as many small grains show evidence for twinning at the TEM scale. However, the fine grain size and the apparent abundance of fluids argue for a component of grain-boundary sliding during deformation (e.g. Schmid *et al.*, 1977). TEM observations demonstrate that twinning continued throughout deformation, with twins overprinting low-angle boundaries and twin boundaries showing evidence of recovery by twin-boundary migration, followed by recrystallization. Twin-boundary migration has been recognized both in naturally (e.g. Vernon, 1981; Burkhard, 1990; Lafrance *et al.*, 1994) and experimentally (e.g. Rutter, 1995) deformed limestone, and Rutter (1995) suggests that twin-boundary migration recrystallization may be a powerful recrystallization mechanism that is rarely preserved in calcite mylonites. The abundance of stylolites and deformed precipitates of calcite observed at the TEM scale suggest that solution-transfer processes were active throughout deformation.

Brittle deformation clearly played an important role in accommodating deformation within the McConnell thrust mylonite. Bedding-parallel, cataclastic, clay seams are common and the presence of folded and dynamically recrystallized calcite veins within these seams demonstrates that brittle deformation was overprinted by crystal-plastic deformation. The bed-parallel clay seams are interpreted to represent a residuum left behind from the dissolution of calcite. Thus, the layering observed in the mylonite is not inherited bedding, rather it is a direct result of dissolution and reprecipitation of calcite driven by thrusting and fluid flow.

Stylolites oriented parallel to bedding and veins are common in the mylonite. The increase in density of the stylolites towards the shear zone, and the abundance of clay seams in the mylonite (and their absence in the damage zone and protolith), suggests that these structures are a result of deformation within the shear zone and are not simply reactivated stylolites that were formed during burial. In addition, there is no evidence to suggest that the majority of stylolites within the shear zone initially formed perpendicular to bedding with subsequent rotation into parallelism with shear zone boundaries. There are three possibilities to explain the vein-parallel geometry of many stylolites: (1) the bed-parallel

stylolites formed essentially as mode II shear fractures, at a low-angle to maximum principal stress (σ_1) within the shear zone; (2) if the stylolites formed as mode I anticracks (Fletcher and Pollard, 1981) σ_3 presumably was oriented at a low angle to bedding during overthrusting; a situation which may occur if the fault was very weak (e.g. Zoback *et al.*, 1987); or (3) a pre-existing anisotropy may influence the orientation of stylolites more than stress orientations within the mylonite. We believe that the anisotropies generated in shear zones have more control on the orientation of the clay seams and the vein-parallel stylolites than do the ambient stress orientations. Late brittle fracturing, represented by thin, discontinuous veins, high-angle normal microfaults and blocky veins perpendicular to bedding generally cross-cut most microstructures. These late, brittle events reflect the deformation within the hanging wall as it moved over the ramp, and partially represent an obviously late, extensional overprint, unrelated to movement along the thrust (e.g. Venter, 1973).

In summary, several deformation mechanisms were active during displacement along the McConnell thrust, including dislocation creep, twinning, solution transfer and cataclasis. Each of these deformation mechanisms contributed significantly to the bulk strain of the mylonite, and each mechanism probably operated throughout much of the displacement, although not continually.

Temperatures during thrusting

Bradbury and Woodwell (1987), based on fluid inclusion analyses of calcite veins and calcite–dolomite geothermometry, suggested that maximum temperatures in the McConnell thrust sheet were of the order of 340°C during thrusting. They attributed these unusually high temperatures (for burial depths < 10 km) to the migration of hot, hinterland-derived fluids which acted to heat up the lowermost part of the Eldon Formation. We find this temperature incompatible with microstructural observations and, furthermore, calcite–dolomite geothermometry of the McConnell thrust mylonites yields variable temperatures, even at the scale of a thin section, ranging from ~ 80 to 400°C (Woodwell, 1985; Kennedy, unpublished data), making interpretation of these data difficult. In addition, given the fast grain-growth kinetics of calcite aggregates, the grain size of the mylonite, if deformed at > 300°C, should be significantly coarser than 1–3 μm (e.g. Olgaard and Evans, 1988; Burkhard, 1990). However, dispersed opaque minerals may act to pin grain boundaries, subsequently inhibiting grain growth, and this may have counteracted the effect of increased temperatures on grain growth (e.g. Olgaard and Evans, 1988; Olgaard, 1990). Detailed temperature evaluation is required in concert with microstructural analyses in order to work out the temperature of formation of the various microstructures at the McConnell thrust mylonite. A conservative estimate is that these mylonites were formed under temperatures of less than 300°C.

Veining, grain-size variations and brittle–ductile deformation

The abundance of thrust-surface-parallel veins and clay seams occurring as packets are striking features of the mylonite. It is proposed that veins were introduced parallel to bedding and underwent progressive deformation by twinning and dislocation creep. After sufficient grain-size reduction by dislocation creep, the fine-grained vein material may have deformed by solution transfer ($\pm$ grain-boundary sliding), however, continual introduction of coarse-grained veins insured that dislocation creep also continued as an important deformation mechanism throughout displacement. Thus, the significance of the matrix veins is that they effectively increased grain size and subsequently promoted dislocation-creep processes within the mylonite; a mechanism that otherwise would probably not have played a key role in the formation of the McConnell thrust mylonite.

In addition to promoting dislocation creep within the mylonite, the thrust-surface-parallel veins indicate that the lithostatic stress (least compressive stress, σ_3) was temporarilly exceeded, presumably by hydrofracturing during intervals of high pore fluid pressures (e.g. Hubbert and Rubey, 1959; also see similar microstructures described by Burkhard *et al.*, 1992). The range in vein deformation from extensively recrystallized to undeformed indicates that vein emplacement (i.e. brittle failure) continued throughout displacement, suggesting a cycling of brittle–ductile deformation and hence deformation mechanisms within the fault zone. The close association of undeformed layer-parallel veins and clay seams and the presence of deformed veins within clay seams suggests that these seams controlled the location of vein emplacement. The interface between clay seams and the calcite matrix represents a planar surface of contrasting rheological properties, and it is at these interfaces that microcracking is expected (e.g. Logan *et al.*, 1973). As a result of this mechanical anisotropy, fluids may migrate along the clay seam–matrix interface, and possibly within the sheared clay seams. The gradual trapping of fluids in the low permeable clay matrix results in localized increases in pore fluid pressures. Thus, the clay seams may represent the loci for brittle failure in an otherwise ductilely deforming rock. The discontinuous geometries of both the veins and clay seams suggest that brittle failure was discontinuous both along and across strike of the mylonite, leading to complex interactions of deformation mechanisms within the mylonite.

Once formed, the clay seams act as layers of weakness, and a significant portion of displacement may have been accommodated intermittently along them during brittle failure. Microstructures, such as the sheared portion of veins restricted to within clay seams, demonstrate that, at least during the latest stages of deformation, the clay

seams accommodated relatively more displacement than the surrounding matrix. Thus, the progressive and continual development of dissolution seams may act essentially as a strain-softening mechanism with displacement localizing along clay seams.

The timing of the calcite vein emplacement is difficult to determine. The relatively undeformed bedding-parallel veins were clearly introduced late in the displacement history; however, whether the dynamically recrystallized veins were introduced while the thrust sheet was still at the lower flat, and therefore at temperatures perhaps as high as 300°C, or later in the transport history under lower temperatures is, as yet, indeterminate. Extensive dislocation creep of calcite aggregates is reported to occur generally in excess of ~280°C (e.g. Burkhard, 1990), although Burkhard (1990) described an example of a calcite mylonite with a strong CPO at temperatures <180°C. Further work directly relating temperatures to microstructures needs to be completed before the question of the temperature under which dynamic recrystallization took place can be adequately addressed.

Our model for the formation of the McConnell thrust mylonite is consistent with that of Bradbury and Woodwell (1987), who, in an extensive oxygen isotope analytic study of the McConnell thrust system, suggested that fluids migrated parallel to the thrust surface from the deeper, more hinterland, portion of the thrust towards the foreland. Bradbury and Woodwell (1987) reported $\delta^{18}O$ values that increase from the hinterland towards the foreland, which they interpreted as a result of progressive interaction between hinterland-derived connate fluids (isotopically light) and carbonate wall rocks (isotopically heavy) as the fluids were channelled and migrated along the fault zone from the hinterland to the foreland. The channelled fluid flow model for the McConnell thrust proposed by Bradbury and Woodwell (1987) is in contrast to the fluid flow geometry interpreted for the Glarus thrust, where Burkhard *et al.* (1992) concluded that fluids were derived by upward migration from the footwall.

Implications for fault-zone rheology

The variety of deformation mechanisms inferred to have operated during thrusting within the McConnell mylonite has implications for the rheology of the fault zone. The interplay between dislocation creep, solution transfer, brittle failure and vein emplacement may have led to spatial and temporal fluctuations in stress across the fault zone. The change in deformation mechanisms is a direct result of both grain size and the development of planar layers of weakness, which are in turn directly related to fluid migration and pore fluid pressure fluctuations within the fault zone. Deformation mechanism maps suggest that under conditions appropriate for the McConnell thrust (e.g. temperatures ranging from ~200 to 300°C) fine-grained calcite will deform at a lower differential stress (by solution-transfer processes ± grain-boundary sliding) than a coarse-grained equivalent (by dislocation creep—e.g. Rutter, 1976, 1995; Walker *et al.*, 1990; Busch and Van Der Pluijm, 1995). Therefore, the continual introduction of coarse-grained calcite may have acted to increase the strength of faults on a long-term basis depending on the relative amounts of fine-grained vs coarse-grained material that existed within the fault zone at a given time. These ambient deformation mechanisms (solution transfer and dislocation creep) were episodically interrupted by brittle failure, triggered by high pore fluid pressures, with subsequent vein emplacement and preferential slip (cataclasis) within clay seams. Significant displacements may have occurred at relatively high strain rates along the clay-rich seams.

SUMMARY AND CONCLUSIONS

At the McConnell thrust, an initially fine-grained, micritic limestone accommodated deformation by a variety of deformation mechanisms, which resulted in the formation of a fine-grained lithologically layered mylonite. Emplacement of coarse-grained calcite veins within the mylonite resulted in extensive operation of dislocation creep and may have had the effect of transiently increasing the strength of the shear zone. Subsequent grain-size reduction of the vein material by dynamic recrystallization promoted the reactivation of grain-size-sensitive processes. Continual emplacement of veins throughout deformation ensured cycling and competition between dislocation creep and solution transfer (± grain-boundary sliding). The presence of undeformed and completely recrystallized veins suggests a cyclicity of brittle failure, triggered by elevated pore fluid pressures, in an otherwise ductilely deforming rock. Dissolution of calcite and the subsequent development of clay-rich seams created a planar anisotropy within the developing mylonite along which preferential displacement occurred. The spatial proximity of clay seams and parallel veins suggests a link between clay-seam generation and the development of local, transient, high pore fluid pressures in fault zones.

Acknowledgements—This research was supported by NSF grant EAR 9316940 and USGS/NEHRP #15-807 awarded to J. M. Logan. We thank J. C. White for helpful discussions throughout the course of this study and for detailed comments on an earlier version of this manuscript. We thank M. Lamberson for creating figure 2 and A. Toma for drafting figure 1. Thoughtful review by E. H. Rutter and J. P. Busch improved the clarity of the paper.

REFERENCES

Angevine, C. L., Turcotte, D. L. and Furnish, M. (1982) Pressure solution lithification as a mechanism for the stick–slip behaviour of faults. *Tectonics* **1**, 151–160.

Barber, D. J. and Wenk, H. R. (1972) The microstructures of experimentally deformed limestones. *Journal of Materials Science* **8**, 500–508.

Behrmann, J. J. (1983) Microstructures and fabric transitions in calcite tectonites from the Sierra Alhamilla (Spain). *Geologische Rundschau* **72**, 605–618.

Blanpied, M. L., Lockner, D. A. and Byerlee, J. D. (1992) An earthquake mechanism based on rapid sealing of faults. *Nature* **358**, 574–576.

Bradbury, H. J. and Woodwell, G. R. (1987) Ancient fluid flow within foreland terranes. In *Flow in Sedimentary Basins and Aquifers*, eds J. C. Goff and B. P. J. Williams, pp. 87–102. Geological Society of America Special Publication **34**.

Burkhard, M. (1990) Ductile deformation mechanisms in micritic limestones naturally deformed at low temperatures (150–350°C). In *Deformation Mechanisms, Rheology and Tectonics*, ed. R. J. Knipe and E. H. Rutter, pp. 241–257. Geological Society of London Special Publication **54**.

Burkhard, M. (1993) Calcite twins, their geometry, appearance and significance as stress–strain markers and indicators of tectonic regime: a review. *Journal of Structural Geology* **15**, 351–368.

Burkhard, M., Kerrich, R., Maas, R. and Fyfe, W. S. (1992) Stable and Sr-isotope evidence for fluid advection during thrusting of the Glarus nappe (Swiss Alps). *Contributions to Mineralogy and Petrology* **112**, 293–311.

Bustin, R. M. (1983) Heating during thrust faulting in the Rocky Mountains: friction or fiction. *Tectonophysics* **95**, 309–328.

Busch, J. P. and Van Der Pluijm, B. A. (1995) Calcite textures, microstructures and rheological properties of marble mylonites in the Bancroft shear zone Ontario, Canada. *Journal of Structural Geology* **17**, 677–688.

Byerlee, J. (1990) Friction, overpressure and fault normal compression. *Geophysical Research Letters* **17**, 2109–2112.

Chapple, W. M. (1978) Mechanics of thin-skinned fold and thrust belts. *Bulletin of the Geological Society of America* **89**, 1189–1198.

Chester, F. M. and Higgs, N. G. (1992) Multimechanism friction constitutive model for ultrafine quartz gouge at hypocentral conditions. *Journal of Geophysical Research* **97**, 1859–1870.

Chester, F. M. and Logan, J. M. (1986) Implications for mechanical properties of brittle faults from observations of the Punchbowl fault zone California. *Pure and Applied Geophysics* **124**, 79–106.

Covey, M. C., Vrolijk, P. J. and Pevear, D. R. (1994) Direct dating of fault movement in the Rocky Mountain Front Ranges of southern Alberta. *Geological Society of America Abstracts with Programs* **26**, A467.

Davis, D., Suppe, J. and Dahlen, F. A. (1983) Mechanics of fold-and-thrust belts and accretionary wedges. *Journal of Geophysical Research* **88**, 1153–1172.

Dietrich, D. and Song, H. (1984) Calcite fabrics in a natural shear environment, the Helvetic nappes of western Switzerland. *Journal of Structural Geology* **6**, 19–32.

Elliott, D. (1976) The motion of thrust sheets. *Journal of Geophysical Research* **81**, 949–963.

Fletcher, R. C. and Pollard, D. D. (1981) Anticrack model for pressure solution surfaces. *Geology* **9**, 419–425.

Fredrich, J. T. and Evans, B. (1992) Strength recovery along simulated faults by solution transfer processes. In *Rock Mechanics*, Proceedings of the 33rd U.S. Symposium, eds J. R. Tillerson and W. R. Wawersik, pp. 121–129.

Friedman, M. and Higgs, N. G. (1981) Calcite fabrics in experimental shear zones. In *Mechanical Behavior of Crustal Rocks—The Handin Volume*, eds. N. L. Carter, M. Friedman, J. M. Logan and D. W. Stearns, pp. 11–27. American Geophysical Union, Geophysical Mongraph 24.

Fyfe, W. S, Price, N. J. and Thompson, A. B. (1978) *Fluids in the Earth's Crust*. Elsevier, New York.

Heitzmann, P. (1987) Calcite mylonites in the Central Alpine "root zone". *Tectonophysics* **135**, 207–215.

Hubbert, M. K. and Rubey, W. W. (1959) Role of fluid pressure in the mechanics of overthrusting faulting. *Bulletin of the Geological Society of America* **70**, 115–166.

Jiang, D. and White, J. C. (1995) Kinematics of rock flow and the interpretation of geological structures, with particular reference to shear zones. *Journal of Structural Geology* **17**, 1249–1266.

Kehle, R. O. (1970) Analysis of gravity sliding and orogenic translation. *Bulletin of the Geological Society of America* **81**, 1641–1664.

Kronenberg, A. K. (1994) Hydrogen speciation and chemical weakening of quartz, In *Silica: Physical Behavior, Geochemistry, and Materials Applications*, eds P. J. Heaney, C. T. Prewitt and J. V. Gibbs, Reviews in Mineralogy Vol. 29, pp. 123–176. Mineralogy Society of America, Washington, DC.

Lafrance, B., White, J. C. and Williams, P. F. (1994) Natural calcite *c*-axis fabrics: an alternate interpretation. *Tectonophysics* **229**, 1–18.

Lister, G. S. and Snoke, A. W. (1984) *S–C* mylonites. *Journal of Structural Geology* **6**, 617–638.

Logan, J. M., Dengo, C. A., Higgs, N. G. and Wang, Z. Z. (1992) Fabrics of experimental fault zones: their development and relationship to mechanical behaviour. In *Fault Mechanics and Transport Properties of Rocks*, ed. T. F. Wong, pp. 33–67. Academic Press, New York.

Logan, J. M., Iwaski, T., Friedman, M. and Kling, S. (1973) Experimental investigation of sliding friction in multilithologic specimens. *Engineering Geology Case Histories* **9**, 55–67.

Marshall, D. J. (1988) *Cathodoluminescence of Geological Materials*. The University Printing House, Oxford.

Meike, A. and Wenk, H.-R. (1988) A TEM study of microstructures associated with solution cleavage in limestone. *Tectonophysics* **154**, 137–148.

Newman, J. and Mitra, G. (1995) Fluid-influenced deformation and recrystallization of dolomite at low temperatures along a natural fault zone, Mountain City window, Tennessee. *Bulletin of the Geological Society of America* **106**, 1267–1280.

Olgaard, D. L. (1990) The role of second phase in localizing deformation. In *Deformation Mechanisms, Rheology and Tectonics*, eds R. J. Knipe and E. H. Rutter, pp. 175–181. Geological Society of London Special Publication **54**.

Olgaard, D. L. and Evans, B. (1988) Grain growth in synthetic marbles with added mica and water. *Contributions to Mineralogy and Petrology* **100**, 246–260.

Price, R.A. and Mountjoy, E.W. (1970) Geologic structure of the Canadian Rocky Mountains between Bow and Athabasca Rivers: A progress report. *Geological Association of Canada, Special Paper* **6**, 7–25.

Rutter, E. H. (1976) The kinetics of rock deformation by pressure solution. *Philosophical Transactions of the Royal Society, London* **A283**, 203–219.

Rutter, E.H. (1995) Experimental study of the influence of stress, temperature, and strain on the dynamic recrystallization of Carrara marble. *Journal of Geophysical Research* **100**, 24651–24663.

Rutter, E. H. and Mainprice, D. H. (1979) On the possibility of slow fault slip controlled by a diffusive mass transfer process. *Gerlands Beiträge Geophysik, Leipzig* **88**, 154–162.

Schmid, S. M., Panozzo, R. and Bauer, S. (1987) Simple shear experiments on calcite rocks: rheology and microfabric. Special research paper. *Journal of Structural Geology* **9**, 747–778.

Schmid, S. M. Casey, M. and Starkey, J. (1981) The microfabrics of calcite tectonites from the Helvetic Nappes (Swiss Alps). In *Thrust and Nappe Tectonics*, eds K. R. Clay, and N. J. Price, pp. 151–158. Geological Society of London Special Publication **9**.

Schmid, S. M. (1976) Rheological evidence for changes in the deformation mechanism of Solnhofen limestone towards low stresses. *Tectonophysics* **31**, 21–28.

Schmid, S. M., Boland, J. N. and Paterson, M. S. (1977) Superplastic flow in fine grained limestone. *Tectonophysics* **43**, 257–291.

Spang, J. H., Brown, S. P., Stockmal, G. S. and Moffat, I. (1981) Structural geology of the Foothills and Front Ranges west of Calgary, Alberta. In *Field Guides to Geology and Mineral Deposits; Calgary 1981 Annual Meeting, GAC/MAC*, eds R. I. Thompson and D. G. Cook, Geological Society, Canada, pp. 101–120.

Stel, H. (1981) Crystal growth in cataclasites: diagnostic microstructures and implications. *Tectonophysics* **78**, 585–600.

Van Der Pluijm, B. A. (1991) Marble mylonites in the Bancroft shear zone, Ontario, Canada: microstructures and deformation mechanisms. *Journal of Structural Geology* **13**, 1125–1135.

Venter, R. H. (1973) McConnell thrust and associated structures at Mount Yamnuska, Alberta, Canada. M.Sc. thesis, University of Calgary.

Vernon, R. H. (1981) Optical microstructure of partly recrystallized calcite in some naturally deformed marble. *Tectonophysics* **78**, 601–612.

Walker, A. N., Rutter, E. H. and Brodie, K. H. (1990) Experimental study of grain size sensitive flow of synthetic, hot-pressed calcite rocks. In *Deformation Mechanisms, Rheology and Tectonics*, eds R. J.

Knipe and E. H. Rutter, pp. 259–284. Geological Society of London Special Publication **54**.

White, S. H. and Knipe, R. J. (1978) Transformation and reaction-enhanced ductility in rocks. *Journal of the Geological Society of London* **135**, 513–516.

Wojtal, S. and Mitra, G. (1986) Strain hardening and strain softening in fault zones from foreland thrusts. *Bulletin of the Geological Society of America* **97**, 674–687.

Wojtal, S. and Pershing, J. (1991) Paleostresses associated with faults of large offset. *Journal of Structural Geology* **13**, 49–62.

Wojtal, S. (1992) One-dimensional models for plane and non-plane power-law flow in shortening and elongating thrust zones. In: *Thrust Tectononics*, ed. K. R. McClay, pp. 41–52. Chapman and Hall, London.

Woodwell, G. R. (1985) Fluid migration in an overthrust sequence of the Canadian Cordillera. Ph.D. thesis, Yale University.

Zoback, M. D., Zoback, M. L., Mount, V., Eaton, J., Healy, J., Oppenheimer, D., Reasonbert, P., Jones, L., Raleigh, B., Wong, I., Scottie, O. and Wentworth, C. (1987) New evidence on the state of stress of the San Andreas fault system. *Science* **238**, 1105–1111.